Advancing surgical guidance: from (hybrid) molecule to man and beyond

Berg, N.S. van den

CHAPTER 4

CONCOMITANT RADIO- AND FLUORESCENCE-GUIDED SENTINEL NODE BIOPSY IN SQUAMOUS CELL CARCINOMA OF THE ORAL CAVITY USING ICG-^{99M}TC-NANOCOLLOID

Adapted from: van den Berg NS*, Brouwer OR*, Klop WMC, Karkullukçu B, Zuur CL, Tan BI, Balm AJM, van den Brekel MWM, Valdés Olmos RA, van Leeuwen FWB. Eur J Nucl Med Mol Imaging. 2012;39:1128-36. * = Shared first authorship.

ABSTRACT

PURPOSE For oral cavity malignancies, sentinel node (SN) mapping is performed by injecting a radiocolloid around the primary tumor followed by lymphoscintigraphy. Surgically SNs can then be localized using a handheld gamma-ray detection probe. The aim of this study was to evaluate the added value of intraoperative fluorescence imaging to the conventional radioguided procedure. For this we used indocyanine green (ICG)-^{99m}Tc-nanocolloid, a hybrid tracer that is both radioactive and fluorescent.

METHODS Fourteen patients with oral cavity squamous cell carcinoma were peritumourally injected with ICG-^{99m}Tc-nanocolloid. SNs were preoperatively identified with lymphoscintigraphy followed by single photon emission computed tomography combined with computed tomography (SPECT/CT) for anatomical localization. During surgery SNs were detected with a handheld gamma-ray detection probe and a handheld near-infrared fluorescence camera. Pre-incision and post-excision imaging with a portable gamma camera was performed to confirm complete removal of all SNs.

RESULTS SNs were preoperatively identified using the radioactive signature of ICG-^{99m}Tc-nanocolloid. Intraoperatively, 43 SNs could be localized and excised with combined radio- and fluorescence guidance. Additionally, in four patients, an SN located close to the primary injection site (in three patients this SN was located in level I) could only be intraoperatively localized using fluorescence imaging. Pathological analysis of the SNs revealed a metastasis in one patient.

CONCLUSION Combined preoperative SN identification and intraoperative radio- and fluorescence guidance during SN biopsy for oral cavity cancer proved feasible using ICG-^{99m}Tc-nanocolloid. The addition of fluorescence imaging was shown to be of particular value when SNs were located in close proximity to the primary tumor.

INTRODUCTION

The incidence of lymph node metastases in patients with squamous cell carcinoma of the oral cavity is 20-30% [1, 2]. By using sentinel node (SN) biopsy to select patients with occult lymph node metastases, an unnecessary elective neck dissection (END) may be avoided in 70-80% of patients [1, 3]. SN biopsy has several advantages over END: (1) reduced morbidity [4]; (2) improved identification of so-called skip metastases and aberrant lymphatic drainage patterns [5-7]; and (3) improved pathological specimen analysis for the detection of (micro-)metastasis [8, 9]. For SN biopsy, overall sensitivity rates of 91% after five-year follow-up have been reported [10]. However, for floor of mouth (FOM) tumors, the sensitivity and the negative predictive values were much lower compared to other sites, 80 vs. 97% and 88 vs. 98%, respectively [10]. A prospective multi-institutional trial reported false-negative rates of 25 and 10% for FOM and tongue tumors, respectively, whereas this was said to be 0% for other types of oral cavity cancers [11]. In oral cavity malignancies, SNs are often located in close proximity to the primary tumor site, which can render SN biopsy difficult.

Conventional SN mapping is performed by injecting a radiocolloid (^{99m}Tc-nanocolloid or ^{99m}Tc-sulphur colloid) in or around the primary tumor followed by sequential lymphoscintigraphy to identify the lymph nodes on a direct drainage pathway from the primary tumor (the SNs) [12]. To provide an overview of the SNs with regard to their anatomical location, single photon emission computed tomography combined with computed tomography (SPECT/CT) was introduced. Additionally, with SPECT/CT more SNs can be visualized compared to conventional lymphoscintigraphy [13]. Intraoperatively, SN localization is commonly guided by the acoustic signal coming from a handheld gamma-ray detection probe (hereafter referred to as gamma probe). However, since for oral cavity cancers SNs are often located in close proximity to the primary tumor site, the high radioactive background signal coming from the injection site may hamper intraoperative radioguidance towards these SNs [6, 14]. Recently, the intraoperative use of a portable gamma camera was shown to improve the localization of SNs near the injection site [15].

Vital blue dyes are generally applied to enable intraoperative visual detection of the SNs, but have shown to be of limited value in oral cavity tumors as SNs in the head-and-neck area are less frequently stained blue compared to other primary tumor sites [16-18]. Moreover, the use of blue dye may blur the visibility of intraoral tumor margins [1, 19].

To enable visual detection of SNs without affecting the surgical field, the near-infrared fluorescence tracer indocyanine green (ICG) was introduced for SN mapping in various tumor types such as breast, colon and gastric cancers [20, 21]. Recently, Bredell evaluated the use of ICG for SN mapping in oropharyngeal cancer [22]. ICG is not visible by the naked eye and does, therefore, not interfere with the visual identification of tumor margins [23]. However, similar to vital blue dyes, ICG rapidly migrates through the lymphatic system leading to a limited diagnostic window and staining of higher-echelon nodes [24]. To address these migratory limitations of optical dyes, the self-assembled hybrid radiocolloid ICG-^{99m}Tc-nanocolloid was clinically introduced for selective SN biopsy [25, 26].

In this complex, ICG adopts the lymphatic migration properties of the radiocolloid, resulting in a significantly longer retention time in the SNs as compared to ICG alone. With this hybrid tracer being both radioactive and fluorescent, preoperative surgical planning can be combined with intraoperative radioguidance towards the SNs. The fluorescent properties of the hybrid tracer extend the radioguided procedure by providing real-time optical localization using an near-infrared fluorescence camera. For head-and-neck melanoma it was shown that with this approach fluorescence-based SN identification was superior over the use of blue dye [26]. The aim of the current study was to explore the utility of the hybrid tracer during SN biopsy for squamous cell carcinoma of the oral cavity.

MATERIALS AND METHODS

PATIENTS

Between May 2011 and January 2012, 14 patients with squamous cell carcinoma of the oral cavity were included in this study after obtaining written informed consent. Patients were scheduled for surgical removal of the primary tumor followed by SN biopsy. All patients were staged with T1/2 tumors and were clinically node negative as assessed by ultrasound and fine-needle aspiration cytology (USFNAC). Further patient characteristics are listed in Table 1. The study protocol was approved by the Institution's Medical Ethics Committee.

TRACER PREPARATION

^{99m}Tc-nanocolloid was prepared by adding 1400 MBq pertechnetate in 2 mL saline to a vial of nanocolloid (GE Healthcare, Eindhoven, The Netherlands). The mixture was then incubated for 30 min at room temperature after which the excess of reactive elements was removed. Before adding ICG, a quality check was performed in which the color, clarity and pH were determined (colourless, clear and pH 6-7, respectively).

ICG was prepared by adding 5 mL sterile water to a vial containing 25 mg ICG (vial concentration 5 mg/mL; Pulsion Medical Systems, Munich, Germany). Then, 50 µL of ICG solution was added to the ^{99m}Tc-nanocolloid to form ICG-^{99m}Tc-nanocolloid.

All procedures were performed under good manufacturing practice (GMP-z) and under supervision of the institution's pharmacist.

TRACER ADMINISTRATION AND PREOPERATIVE IMAGING

A median of 77 MBq (range 67-94 MBq) ICG-^{99m}Tc-nanocolloid was injected in three or four deposits around the primary tumor (total volume 0.4 mL; Figure 1). To visualize the lymphatic duct(s) with the subsequent SN(s), anterior and lateral dynamic images were obtained during the first 10 min after injection using a dual-head gamma camera (Symbia T, Siemens, Erlangen, Germany). Static planar gamma camera images were acquired 15 min and 2 h post-injection (Figure 2A). The latter was immediately followed by SPECT/CT

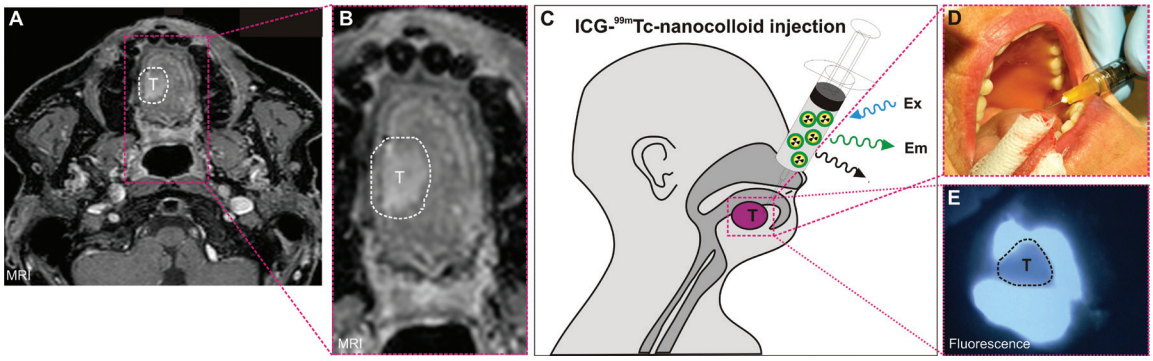

Figure 1. Hybrid ICG-^{99m}Tc-nanocolloid injection. A) Axial diagnostic MRI image showing a tumor on the tongue (T); B) Zoom in on the tongue tumor; C-D) ICG-^{99m}Tc-nanocolloid is peritumourally injected in three to four deposits; E) Intraoperative, near-infrared fluorescence-based visualization of the injection site and tumor (T). MRI = magnetic resonance; ICG = indocyanine green; Ex = exitation light; Em = emission light.

imaging (Symbia T, Siemens, Erlangen, Germany; Figure 2B). SPECT and CT images were obtained on the basis of 2 mm slices. After tissue attenuation correction for the SPECT, fused SPECT/CT images were generated. SPECT, CT and fused SPECT/CT images were simultaneously evaluated using orthogonal multiplanar reconstruction. In addition, three-dimensional (3D) display using volume rendering was performed in order to im-prove anatomical neck level recognition (Figure 2C).

SNs were defined as the lymph nodes on a direct lymphatic drainage pathway from the primary tumor [12]. Early draining lymph nodes in a basin were considered to be the SNs in case of multiple visualized lymph nodes without visible afferent vessels.

SURGICAL PROCEDURE

SN biopsy started 3-19 h after ICG-^{99m}Tc-nanocolloid administration. In the operating room, a portable gamma camera (Sentinella equipped with Sentinella suite software version 7.5; Oncovision, Valencia, Spain) was used to acquire a pre-incision overview image (Figure 3B, pre-incision) and to determine the location for the incision(s) [15]. Initial SN exploration was guided by a gamma probe (Neoprobe, Johnson & Johnson Medical, Hamburg, Germany; Figure 3D). Fluorescence imaging with a dedicated handheld near-infrared fluorescence camera (PhotoDynamic Eye, Hamamatsu Photonics K.K., Hamamatsu, Japan; Figure 3E) was performed to optically detect the SNs. After excision of the SN(s), the portable gamma camera was used to search for remaining radioactive hot spots in the SN excision area (Figure 3B, post-excision) as was previously described by Vermeeren et al. [15]. Higher-echelon nodes (defined by preoperative lymphoscintigraphy and SPECT/ CT) were left in situ.

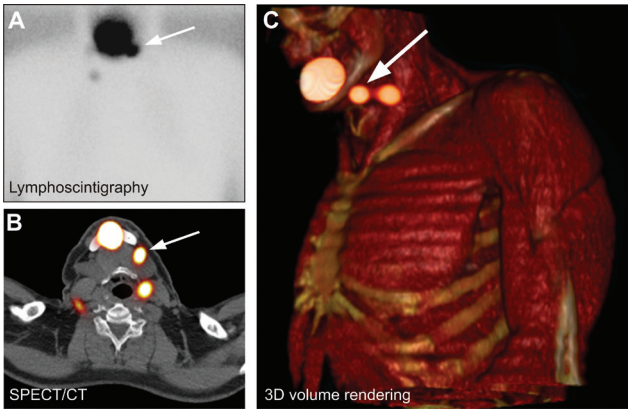

Figure 2. Preoperative sentinel node identification. A) Late planar anterior lymphoscintigram acquired 2 h post-injection showing two SNs on the right side and one SN on the left side (arrow); B) Axial SPECT/CT slice showing two level II SNs (bilateral) and a level I SN close to the injection site (arrow); C) The 3D volume-rendered SPECT/CT showing two SNs on the left side, in level I (arrow) and level II (these SNs were not visible as separate hot spots on the planar lymphoscintgram). 3D = three-dimensional; SPECT/CT = single photon emission computed tomography/computed tomography.

PATHOLOGY

Harvested SNs were fixed in formalin, bisected, embedded in paraffin, cut at a minimum of six levels at 50-150 µM intervals and histologically evaluated for the presence of (micro-) metastases (haematoxylin and eosin (H&E) and anti-cytokeratin (CAM 5.2; Becton Dickinson, San Jose, CA, USA) staining).

RESULTS

PREOPERATIVE FINDINGS

Distribution of the tumor locations of the 14 included patients was as follows: FOM (n=5), tongue (n=7), lower lip (n=1) and buccal mucosa (n=1). Further patient characteristics, and the pre- and intraoperative findings of all 14 patients are outlined in Table 1. A schematic overview of primary tumor and intraoperative SN location is provided in Figures 4A and B, respectively.

Lymphatic drainage was visualized in all patients. Bilateral lymphatic drainage was found in eight patients. In only three of these patients (patients 1, 12 and 14) the tumor had crossed the midline. Using conventional lymphoscintigraphy, a total of 37 SNs were visualized. Four additional SNs were only visible on the SPECT/CT images in three patients (patients 8, 9 and 12) resulting in a total of 41 preoperatively defined SNs (median of 3 SNs per patient; range 1-5) dispersed over 34 basins (median of two basins per patient; range 1-5 basins per patient) (Table 1). In all 14 patients, the fused SPECT/CT images provided an accurate anatomical reference point for surgical planning of the SN biopsy procedure, including the SNs that were found to be located close to the primary injection site (an example is given in Figure 2).

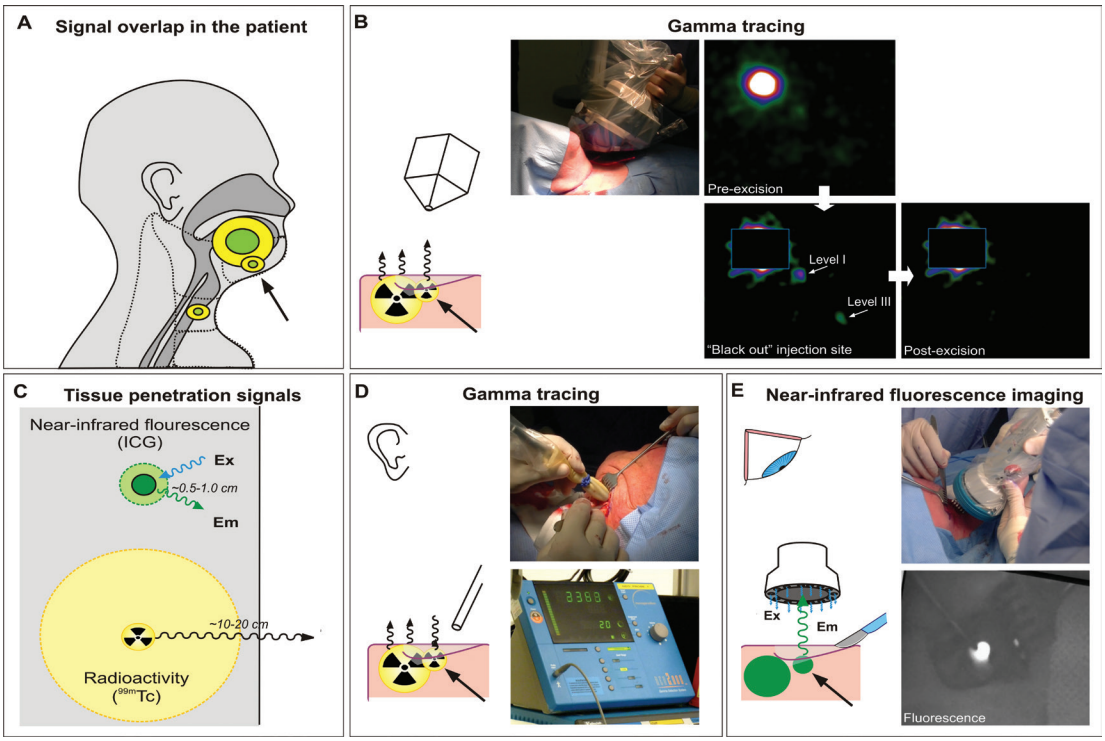

Figure 3. Intraoperative sentinel node identification. A) Schematic overview depicting how detection of an SN residing close to the primary tumor/injection site (arrow) can be difficult with radioguidance alone because of the high background signal coming from the injection site; B) Intraoperative gamma imaging with a portable gamma camera is performed before and after excision of the SN(s) to localize and to confirm complete removal of all predetermined SNs, respectively. The "blackout zone" feature of the portable gamma camera enables masking of the primary injection site, increasing the signal intensities of the weaker radioactive hot spots; C) The fluorescence signal penetration depth of the near-infrared fluorescent dye ICG is limited to approximately 0.5-1.0 cm, whereas the penetration depth of the radioactive signal is much greater depending on the imaging modality used; D) Intraoperatively, SNs are acoustically traced with a gamma probe; E) Near-infrared fluorescence imaging allows for visual identification and excision of the SN(s). Ex = excitation; Em = emission; Tc = technetium; ICG = indocyanine green; SN = sentinel node.

Table 1. Patient characteristics

					Preoperative imaging		Intraoperative findings				Pathology
Pt	*Age (years)*	*Sex*	*Tumor location*	*Time injection - surgery (h)*	*Total # defined SNs*	*SN location*	*Radio guidance*	*Fluore-scence guidance*	*Total # excised SNs*	*Location additional excised SNs*	*Tumor-positive nodes*
1	61	M	FOM midline	4	2	R level III; L level III	3	3	3	R level III	0
2	51	M	Tongue R	5	2	R level I, level III	2	2	2		0
3	58	F	FOM L	19	2	L level I, level III	3	3	3	L level III	0
4	62	F	Tongue R	5	3	R level I, level II; L level III	3	3	3		0
5	59	F	Tongue R	4	2	R level II, level III	1	2	2		1
6	84	F	Buccal mucosa R	19	1	R level II	1	1	1		0
7	82	M	Tongue L	19	3	L level II, 2xlevel III	-§	-§	0		-
8	74	M	Lower lip L	5	5	R level III L 3xlevel I, level III	7	7	7	L 2x level I	0
9	61	F	FOM R	4	4	L 2xlevel III, level I; R level III	3	4	4		0
10	65	M	Tongue R	4	4	R level I, level II; L level II, level III	4*	4*	4*	R level II	0
11	75	M	Tongue L	4	1	L level II	3	3	3	L 2x level II	0
12	60	M	FOM midline	4	4	L level I, level III; R level III, level IV	5	6	6	R 2x level III	0
13	71	M	Tongue R	3	3	R level II; L level III, level V	3	3	3		0
14	54	F	FOM midline	4	5	L level I, level III; R level I, level II, level III	5	6	6	L level I	0
Total					41		43	47	47		1

§ In this patient, the SN procedure was ceased. * In this patient, the L level II SN was not excised. SN = sentinel node; LN = lymph node; M = male; F = female; FOM = floor of mouth; R = right; and L = left.

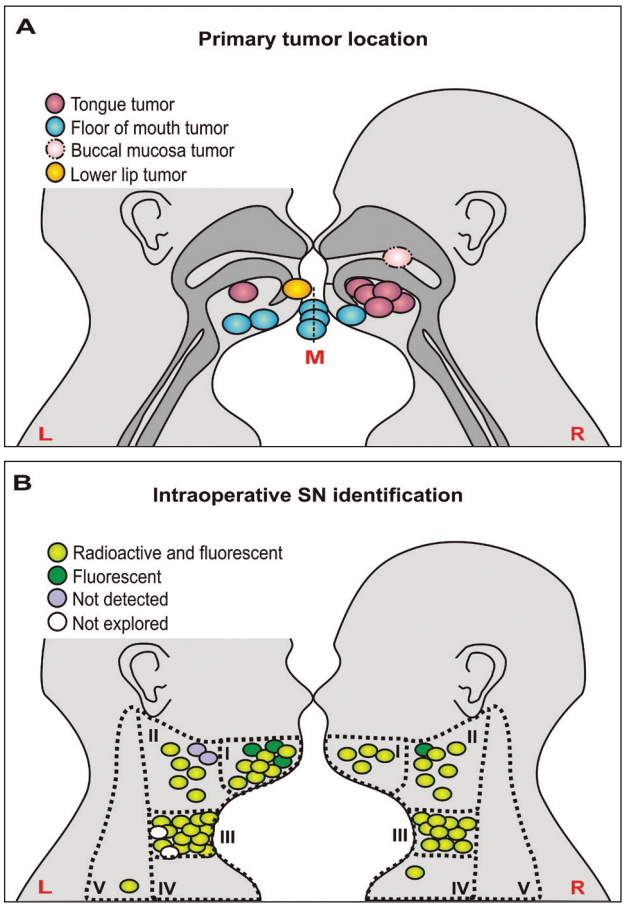

Figure 4. Schematic overview of primary tumor location and the intraoperative sentinel node identification results. A) Primary tumor location; B) Intraoperative SN identification method. The nodes that could be best identified with near-infrared fluorescence imaging during surgery (green dots in the figure) were also radioactive. L = left; R = right; M = midline. SN = sentinel node.

INTRAOPERATIVE FINDINGS

The SN biopsy procedure started 3-19 h post-ICG-^{99m}Tc-nanocolloid-injection and could be completed in all but two patients (patients 7 and 10; Table 1). A total of 47 SNs (median of three SNs per patient; range 0-7) was intraoperatively detected and excised; 43 SNs could be intraoperatively localized with the combined radio- and fluorescence guidance approach (Figure 4B). In four patients (patients 5, 9, 12 and 14), a total of four SNs were found to be located close to the injection site (level I or II; Table 1, Figure 4B). In these patients, SN identification with the gamma probe was hampered due to the high background signal coming from the injection site (Figure 3). Although the portable gamma camera was able to distinguish these SNs from the injection site after masking the injection site using the "blackout zone" function (Figure 3B), fluorescence imaging proved to be the most accurate technology for the identification of these SNs during surgery. To optimize fluorescence-based SN identification, lights were dimmed in the operating room. The SNs could be

pointed out or taken hold of with a surgical forceps (Figure 3E). Subsequently, the light was turned back on and the SN could be excised.

In four patients (patients 3, 8, 10 and 12), a total of 7 additional SNs were identified with the gamma probe. These SNs were not previously identified as separate hot spots on the preoperative images (most probably these SNs were part of a cluster of SNs). These nodes also proved to be fluorescent and were subsequently harvested. Post-excision control with the portable gamma camera revealed residual radioactivity in the excision area in three patients (patients 1, 11 and 14). This resulted in the removal of three additional SNs, again guided by a combination of gamma probe tracing and fluorescence imaging.

In two patients, the SN biopsy procedure was not completed to prevent possible vital structure damage. In patient 7 an SN was located medially of the mandible and very close to the main trunk of the facial nerve (Supporting information Figure SI1). Despite successful detection with the gamma probe and the portable gamma camera, visualization of this SN with the near-infrared fluorescence camera was not possible. In patient 10, an SN was located near branches of the marginal mandibular nerve. This SN could be detected with the portable gamma camera, but its exact location could not be identified with the gamma probe. Initial exploration with the near-infrared fluorescence camera also did not reveal the location of the SN. To reduce the invasiveness of the procedure and to prevent the possible risk of paresis of the lower lip, it was decided not to proceed with the excision. In both cases, the lack of a fluorescent signal suggested that the SN left in situ was located >0.5 cm deeper from the surface imaged; the penetration depth of ICG is limited to 0.5-1.0 cm (Figure 3). Both patients will be closely monitored following the “watch and wait” protocol.

PATHOLOGICAL FINDINGS

Although the SNs were clearly defined in vivo by fluorescence imaging, it was impossible to solely dissect the single SN separately in five patients (patients 1, 5, 8, 10 and 13). Subsequently, in these patients some additional tissue was also excised. This resulted in the identification of 13 additional lymph nodes in these tissue specimens. All of these lymph nodes were evaluated as SNs.

Histopathological examination revealed SNs with largest diameters varying from two to 25 mm with a median of 6 mm. In one patient (patient 5) a level III lymph node metastasis of 3 mm was found. This patient received a subsequent therapeutic neck dissection in which 34 additional tumor-negative lymph nodes from level I-V were removed.

DISCUSSION

The present study shows that a single injection of ICG-^{99m}Tc-nanocolloid enables preoperative SN mapping and intraoperative radio- and fluorescence-guided identification of the SNs draining from primary oral cavity cancers. SPECT/CT and the portable gamma camera allowed for accurate surgical planning, even when SNs were found in close proximity to the injection site. Intraoperatively, surgeons experienced the optical detection of the SNs provided by the fluorescent label of the hybrid tracer as valuable, especially in cases where localization with the gamma probe was impeded by high radioactive background signals. In FOM tumors, SN biopsy is discouraged due to its low sensitivity [10], which we reason may partially be a result of the difficulty to intraoperatively localize such SNs in the vicinity of the injection site. The addition of fluorescence imaging to the conventional radioguided procedure may be of particular benefit in this patient group. In this study, a total of four SNs were found in level I in the five patients with FOM tumors. Three (75%) of these could only be accurately detected with fluorescence imaging.

Contralateral lymph node involvement ranges from 0.9 to 34.7% [27]. Bilateral lymphatic drainage was observed on the lymphoscintigrams in 54% of patients (n=8), even though the primary tumor had crossed the midline in only three of these patients. Hence, by performing an upfront unilateral END, such (potentially tumor-positive) contralateral draining nodes might be missed.

With the rise of minimally invasive surgery, SN biopsy becomes more favorable over END procedures. Lymph nodes are generally small (3-4 mm) and are frequently found in close proximity to each other [18]. These conditions create high demands on the limited spatial resolution of the gamma probe. In the current study, the high spatial resolution (down to the micrometer level) provided by fluorescence imaging enabled the detection and removal of individual SNs as small as 2 mm.

The use of a non-covalent self-assembly approach to generate imaging agents is appealing as it allows for the formation of hybrid agents by combining “simple” and often commercially available, clinically approved building blocks [28]. The hybrid tracer ICG-^{99m}Tc-nanocolloid was built from ^{99m}Tc-nanocolloid particles (used for conventional SN mapping in Europe) and the near-infrared fluorescent dye ICG. Good manufacturing practice (GMP-z)-based preparation of ICG-^{99m}Tc-nanocolloid only adds one additional step to the conventional radiocolloid preparation process, namely the addition of 0.25 mg ICG to a solution of fully prepared ^{99m}Tc-nanocolloid. The pH of the ^{99m}Tc-nanocolloid solution is 6-7, and therefore the preparation protocol does not negatively influence the optical properties of ICG [29]. With this hybrid approach SNs could be accurately visualized using approximately 100 times lower quantities of ICG compared to the study of Bredell [22]. Although one may reason that non-covalent particles may disintegrate in vivo, a large degree of signal overlap was found in the lymphatic system in both preclinical models [24, 30, 31] and in patients [25, 26]. In none of our clinical studies performed thus far did we find nodes that solely contained a fluorescent or a radioactive signal [25, 26].

The use of ICG alone for SN mapping of oropharyngeal cancer was set to be optimal 5 min post-ICG-injection [22], while in the current study SNs were still fluorescent at 19 h after ICG-^{99m}Tc-nanocolloid injection. Clearly the retention of the hybrid tracer in the SNs yields a superior diagnostic window. It therefore does not require additional (intraoperative) injections which helps to optimize the logistics in daily practice. The limited penetration depth of fluorescence imaging compared to modalities based on radioactivity may even be useful, since it can help the surgeon to estimate the depth at which an SN can be localized in order to decide if further exploration is needed (as described for patients 7 and 10). The near-infrared fluorescence signal coming from ICG is invisible to the naked eye and can only be visualized with a dedicated near-infrared fluorescence camera system. As such ICG does not interfere with primary tumor margin visibility [23] like blue dyes do. This study demonstrates how optical guidance provided by the hybrid tracer's fluorescent label offers an excellent alternative over visual blue dyes and facilitates accurate SN localization, even when an SN resides in close proximity to the primary tumor.

Supplementing the conventional radioguided SN biopsy procedure with fluorescence only moderately increases the costs of the procedure as the near-infrared fluorescence imaging system used in this study is in the same price range as a gamma probe. The costs of ICG are also not higher than that of the original tracer ^{99m}Tc-nanocolloid and one vial of ICG can be used for multiple tracer preparations.

CONCLUSION

The hybrid tracer ICG-^{99m}Tc-nanocolloid allows for both preoperative lymphatic mapping and intraoperative SN detection up to 19 h post-injection. The added guidance provided by fluorescence imaging proved especially valuable for the detection of SNs located close to the primary tumor site.

REFERENCES

1. Broglie MA, Stoeckli SJ. Relevance of sentinel node procedures in head and neck squamous cell carcinoma. Q J Nucl Med Mol Imaging. 2011;55:509-20.
2. Coughlin A, Resto VA. Oral cavity squamous cell carcinoma and the clinically n0 neck: the past, present, and future of sentinel lymph node biopsy. Curr Oncol Rep. 2010;12:129-35.
3. Stoeckli SJ, Alkureishi LW, Ross GL. Sentinel node biopsy for early oral and oropharyngeal squamous cell carcinoma. Eur Arch Otorhinolaryngol. 2009;266:787-93.
4. Murer K, Huber GF, Haile SR, Stoeckli SJ. Comparison of morbidity between sentinel node biopsy and elective neck dissection for treatment of the n0 neck in patients with oral squamous cell carcinoma. Head Neck. 2011;33:1260-4.
5. Byers RM, Weber RS, Andrews T, McGill D, Kare R, Wolf P. Frequency and therapeutic implications of "skip metastases" in the neck from squamous carcinoma of the oral

tongue. Head Neck. 1997;19:14-9.
6. Civantos FJ, Moffat FL, Goodwin WJ. Lymphatic mapping and sentinel lymphadenectomy for 106 head and neck lesions: contrasts between oral cavity and cutaneous malignancy. Laryngoscope. 2006;112:1-15.
7. Stoeckli SJ. Sentinel node biopsy for oral and oropharyngeal squamous cell carcinoma of the head and neck. Laryngoscope. 2007;117:1539-51.
8. Civantos Jr F, Zitsch R, Bared A, Amin A. Sentinel node biopsy for squamous cell carcinoma of the head and neck. J Surg Oncol. 2008;97:683-90.
9. Stoeckli SJ, Pfaltz M, Ross GL, Steinert HC, MacDonald DG, Wittekind C, et al. The second international conference on sentinel node biopsy in mucosal head and neck cancer. Ann Surg Oncol. 2005;12:919-24.
10. Alkureishi LW, Ross GL, Shoaib T, Soutar DS, Robertson AG, Thompson R, et al. Sentinel node biopsy in head and neck squamous cell cancer: 5-year follow-up of a European multicenter trial. Ann Surg Oncol. 2010;17:2459-64.
11. Civantos FJ, Zitsch RP, Schuller DE, Agrawal A, Smith RB, Nason R, et al. Sentinel lymph node biopsy accurately stages the regional lymph nodes for T1-T2 oral squamous cell carcinomas: results of a prospective multi-institutional trial. J Clin Oncol. 2010;28:1395-400.
12. Nieweg OE, Tanis PJ, Kroon BB. The definition of a sentinel node. Ann Surg Oncol. 2001;8:538-41.
13. Vermeeren L, Valdés Olmos RA, Klop WM, van der Ploeg IM, Nieweg OE, Balm AJ, et al. SPECT/CT for sentinel lymph node mapping in head and neck melanoma. Head Neck. 2011;33:1-6.
14. de Bree R, Leemans CR. Recent advances in surgery for head and neck cancer. Curr Opin Oncol. 2010;22:186-93.
15. Vermeeren L, Valdés Olmos RA, Klop WM, Balm AJ, van den Brekel MW. A portable gamma-camera for intraoperative detection of sentinel nodes in the head and neck region. J Nucl Med. 2010;51:700-3.
16. Chao C, Wong SL, Edwards MJ, Ross MI, Reintgen DS, Noyes RD, et al. Sentinel lymph node biopsy for head and neck melanomas. Ann Surg Oncol. 2003;10:21-6.
17. Eicher SA, Clayman GL, Myers JN, Gillenwater AM. A prospective study of intraoperative lymphatic mapping for head and neck cutaneous melanoma. Arch Otolaryngol Head Neck Surg. 2002;128:241-6.
18. Tanis PJ, Nieweg OE, van den Brekel MW, Balm AJ. Dilemma of clinically node-negative head and neck melanoma: outcome of “watch and wait” policy, elective lymph node dissection, and sentinel node biopsy-a systematic review. Head Neck. 2008;30:380-9.
19. Kuriakose MA, Trivedi NP. Sentinel node biopsy in head and neck squamous cell carcinoma. Curr Opin Otolaryngol Head Neck Surg. 2009;17:100-10.
20. Polom K, Murawa D, Rho YS, Nowaczyk P, Hünerbein M, Murawa P. Current trends and emerging future of indocyanine green usage in surgery and oncology: a literature review. Cancer. 2011;117:4812-22.

21. Schaafsma BE, Mieog JS, Hutteman M, van der Vorst JR, Kuppen PJ, Löwik CW, et al. The clinical use of indocyanine green as a near-infrared fluorescent contrast agent for image-guided oncologic surgery. J Surg Oncol. 2011;104:323-32.
22. Bredell MG. Sentinel lymph node mapping by indocyanin green fluorescence imaging in oropharyngeal cancer - preliminary experience. Head Neck Oncol. 2010;2:31.
23. Vahrmeijer AL, Frangioni JV. Seeing the invisible during surgery. Br J Surg. 2011;98:749-50.
24. van Leeuwen AC, Buckle T, Bendle G, Vermeeren L, Valdés Olmos R, van de Poel HG, et al. Tracer-cocktail injections for combined pre- and intraoperative multimodal imaging of lymph nodes in a spontaneous mouse prostate tumor model. J Biomed Opt. 2011;16:016004.
25. van der Poel HG, Buckle T, Brouwer OR, Valdés Olmos RA, van Leeuwen FW. Intraoperative laparoscopic fluorescence guidance to the sentinel lymph node in prostate cancer patients: clinical proof of concept of an integrated functional imaging approach using a multimodal tracer. Eur Urol. 2011;60:826-33.
26. Brouwer OR, Klop WM, Buckle T, Vermeeren L, van den Brekel MW, Balm AJ, et al. Feasibility of sentinel node biopsy in head and neck melanoma using a hybrid radioactive and fluorescent tracer. Ann Surg Oncol. 2012;19:1988-94.
27. González-Garcia R, Naval-Gías L, Rodríguez-Campo FJ, Sastre-Pérez J, Muñoz-Guerra MF, Gil-Díez Usandizaga JL. Contralateral lymph neck node metastasis of squamous cell carcinoma of the oral cavity: a retrospective analytic study in 315 patients. J Oral Maxillofac Surg. 2008;66:1390-8.
28. Buckle T, Chin PT, van Leeuwen FW. (Non-targeted) radioactive/fluorescent nanoparticles and their potential in combined pre- and intraoperative imaging during sentinel lymph node resection. Nanotechnology. 2010;21:482001.
29. Björnsson OG, Murphy R, Chadwick VS, Björnsson S. Physiochemical studies on indocyanine green: molar lineic absorbance, pH tolerance, activation energy and rate of decay in various solvents. J Clin Chem Clin Biochem. 1983;21:453-8.
30. Buckle T, van Leeuwen AC, Chin PT, Janssen H, Muller SH, Jonkers J, et al. A self-assembled multimodal complex for combined pre- and intraoperative imaging of the sentinel lymph node. Nanotechnology. 2010;21:355101.
31. Bunschoten A, Buckle T, Kuil J, Luker GD, Luker KE, Nieweg OE, et al. Targeted non-covalent self-assembled nanoparticles based on human serum albumin. Biomaterials. 2012;33:867-75.

SUPPORTING INFORMATION

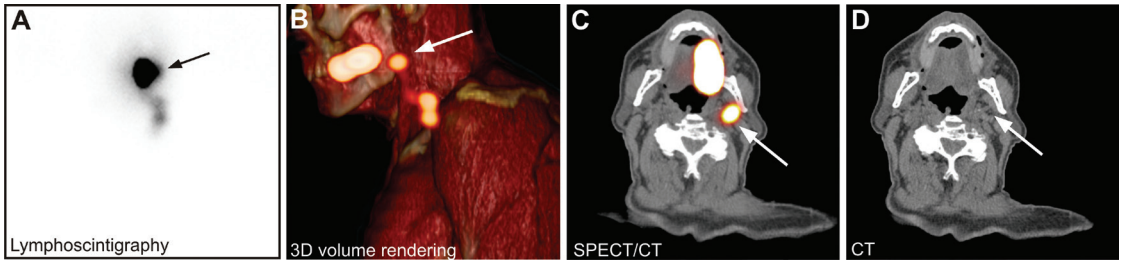

Figure SI1. Preoperative sentinel node mapping (patient 7). A) Anterior planar lymphoscintigram 2 h post-injection vaguely showing three SNs; B) 3D volume-rendered SPECT/CT image confirming the lymphoscintigraphic findings and adding anatomical information; C) Axial fused SPECT/CT image showing the SN located medially of the mandible (arrow) very close to the main trunk of the facial nerve. D) The corresponding SN can be distinguished on the CT image (arrow). SN = sentinel node; 3D = three-dimensional; SPECT/CT = single photon emission computed tomography combined with computed tomography.